Article

Influence of an Automated Vehicle with Predictive Longitudinal Control on Mixed Urban Traffic Using SUMO

Paul Heckelmann *[ID] and Stephan Rinderknecht [ID]

Institute for Mechatronic Systems, Technical University of Darmstadt, 64289 Darmstadt, Germany; rinderknecht@ims.tu-darmstadt.de
* Correspondence: paul.heckelmann@tu-darmstadt.de

Abstract: In this paper, an approach to quantify the area of influence of an intelligent longitudinally controlled autonomous vehicle in an urban, mixed-traffic environment is proposed. The intelligent vehicle is executed with a predictive longitudinal control, which anticipates the future traffic scenario in order to reduce unnecessary acceleration. The shown investigations are conducted within a simulated traffic environment of the city center of Darmstadt, Germany, which is carried out in the traffic simulation software "Simulation of Urban Mobility" (SUMO). The longitudinal dynamics of the not automated vehicles are considered with the Extended Intelligent Driver Model, which is an approach to simulate real human driver behavior. The results show that, in addition to the energy saving caused by a predictive longitudinal control of the ego vehicle, this system can also reduce the consumption of surrounding traffic participants significantly. The area of influence can be quantified to four vehicles and up to 250 m behind.

1. Introduction

With the increase in computing power and major breakthroughs in the topic of autonomous vehicles (AV), the path to fully and connected AVs is set [1]. The transformation of traffic towards full autonomy results also in a change in traffic behavior. According to [2] the transformation to fully autonomous traffic will have positive effects on traffic flow and traffic capacity. However, the development of fully autonomous traffic will take a significant amount of time and will involve mixed traffic scenarios. Also, it is expected that the share of AVs in urban areas will increase slowly compared to highway situations due to the more complex traffic situations in cities [3,4].

With the increasing efforts reducing the energy demand of the transportation sector, and an expected increase in AVs in future traffic, also AVs must be designed as efficiently as possible to fulfill this goal. One part of this task is a minimum energy consumption during the production of the vehicles and an optimized drivetrain for the corresponding use case [5]. Also, by an efficient drive strategy, AVs can save energy and emissions. This aspect is mainly affected by the longitudinal motion of a vehicle. For the longitudinal control of AVs, current research is mainly focused on maintaining safety [6] for all possible traffic situations or improving the throughput [7], but also first approaches on increasing the efficiency of an Intelligent Controlled automated Vehicle (ICV) within a chosen traffic scenario are made.

Karkan et al. [8] and Yang et al. [9] are considering a Cooperative Adaptive Cruise Control system for an efficient longitudinal control. These contributions are both using different types of Vehicle-to-everything (V2X)-information. In addition, Karkan et al. [8] is also investigating the market share of V2X information available for an ICV but is not including the surrounding vehicles' consumption. Walz [10] and Morlock et al. [11] are using MPC approaches for the control of the longitudinal motion of a vehicle, these are also

showing potential for reducing the energy consumption of the ego vehicle but are inflicted by a comparatively high required computing power.

Patella et al. [12] are focusing more on the environmental impact of the life cycle of AVs. Even though no specific longitudinal control approach is shown in this work, a major reduction in energy consumption within the operation phase is forecasted. Here, no mixed traffic scenarios are investigated, but a lower energy consumption of the whole fleet is projected due to more efficient traffic behavior.

Eichenlaub et al. [13,14] are using an intelligent, predictive longitudinal control approach, which is based on state-of-the-art speed and headway control modes but extends these by further elements, which are explained in detail in Section 2.

In the shown longitudinal control approaches, the main objective is the increased energy efficiency of the ego vehicle, by maintaining safety. Additional to that, impacts to other traffic participants, which are Human Controlled Vehicles (HCV), can also be expected in mixed traffic scenarios. The extent of this impact has not yet been focused on in previous research and is an additional positive effect on the evaluation of such intelligent, predictive longitudinal control systems.

So far, the main focus of the investigations in mixed traffic scenarios is the view on the marked share of AVs and following this, researchers are just taking into account the consumption of the AVs, not referring to the consumption of the also operating HCV. These results are additionally also very much dependent on the viewed traffic scenario. To estimate the impact of an ICV on a not-specified traffic situation, the area of influence around an ICV in an urban traffic environment to other HCVs is evaluated for urban traffic in this paper. With the insight of this paper, the marked share behavior of ICV can be explained and forecasted for different traffic scenarios, which was not possible for this form before.

To investigate the potential of an ICV and its influence on other traffic participants and also including connected infrastructure elements, which are not yet available in real traffic environments, the following results are based on a simulative approach with a co-simulation environment, which is described in Section 2.

This paper is organized as follows: as explained, Section 2 contains the co-simulation environment and Section 3 explains the experimental approach. Section 4 concludes with the results and Section 5 with the conclusion.

2. Co-Simulation Environment

The co-simulation environment includes two parts, which are shown in Figure 1. The traffic simulation is executed with the traffic simulation software SUMO (version 1.19.0), which provides a microscopic, internal and multimodal, time-discrete traffic flow platform [15]. SUMO provides the option to control and access the data of every vehicle individually. This allows the interaction of a vehicle simulation with the traffic simulation.
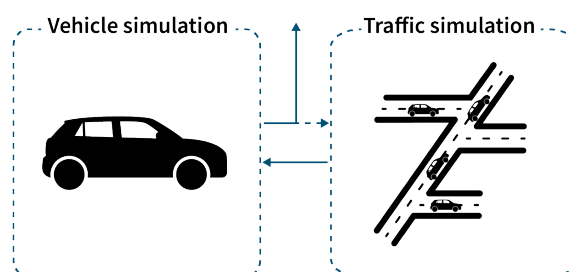

Figure 1. Co-simulation environment with vehicle and traffic simulation.

For this paper, the SUMO simulation is executed with a street network of the city center of Darmstadt, Germany, which is shown in Figure 2. The time step size is 0.2 s, which allows a highly frequent data collection and, if executed, a small interval between two speed-controlled points in time.

Figure 2. Map of the traffic simulation environment (city center of Darmstadt, Germany) with traffic scenario R.

To calculate the vehicles' energy consumption, a backward-facing longitudinal dynamics model is used. The necessary energy is determined based on driving resistance equations to provide the desired vehicle speed. To calculate the longitudinal behavior of the shown vehicles, the dynamic system behavior of the drivetrain can, according to [16,17], be taken into account with a first-order lag element, which is shown in Equation (1).

$$H_{FZ}(s) = \frac{a}{a_{\text{set}}} = \frac{K_{FZ}}{\tau_{FZ}s + 1} \tag{1}$$

Here, a is the executed acceleration and a_{set} the desired acceleration according to the longitudinal dynamics control, which is executed. The used approaches are shown in Sections 2.1 and 2.2. The gain factor is chosen as $K_{FZ} = 1$ and the time constant is chosen as $\tau_{FZ} = 0.2$. According to [18,19], these values characterize the dynamic behavior of an electric powertrain sufficiently. With this, the necessary traction force F_{tr} can be calculated with Equation (2)

$$F_{tr} = m_{\text{eff}}a + \frac{1}{2}c_w A_{Fz}\rho v^2 + c_r mg \cos \alpha_s + mg \sin \alpha_s \tag{2}$$

In this Equation, the rotational inertia of the drivetrain is being neglected to simplify, so $m_{\text{eff}} = m$. The value for ρ represents the air density and α_s the current slope in the direction of driving. The speed of the vehicle v is directly resulting from the previous speed and the acceleration a. The values for the drag coefficient c_w, the rolling resistance coefficient c_r and the frontal surface of the vehicle A_{Fz} and the vehicle mass m are shown in Table 1.

Table 1. Main vehicle parameters.

Vehicle Parameters	Vehicle
Vehicle mass m	1500 kg
Drag coefficient c_w	0.3
frontal surface of the vehicle A_{Fz}	3.6 m^3
Rolling resistance coefficient c_r	0.0075
EM max. torque	350 Nm
EM max. speed	900 Nm

With this, the braking torque T_{br} and the tire radius r, the resulting Moment of the electric motors T_{EM} can be calculated with Equation (3).

$$T_{\text{EM}} = F_{\text{tr}} r - T_{\text{br}} \tag{3}$$

The efficiency level of the powertrain depends on the current operation point. This efficiency is also taken into account within the executed vehicle simulation and needs to be included in T_{EM}. Also, recuperation is implemented in the vehicle simulation. Only if the desired torque for deceleration exceeds the maximal recuperation torque, the mechanical brakes dissipate the excess energy with T_{br}. Refer to Eßer et al. [20] for a more detailed description of the powertrain model calculation. This approach is a common way to model the consumption of electric vehicles as also used in [21].

For the investigation of this paper, a powertrain layout is chosen based on an exemplary design for an AV in urban areas. According to Kraus et al. [22], an all-wheel drive wheel hub powertrain design is suitable for this use case. This type of drivetrain layout is also discussed in [23,24] and is considered favorable in urban traffic. One example of an AV, which is already constructed and operating for test use cases, is the *EDAG CityBot* This vehicle is designed as a battery electric vehicle with wheel hub direct drive electric machines (EM) in all four wheel hubs [24,25]. To maximize the overall efficiency of the four EMs, an operational strategy is implemented that optimizes the use of each EM for optimized vehicle efficiency. This powertrain design is used for both the ICV and HCV to compare all vehicles' consumption based on the driving behavior without being inflicted by different vehicle and powertrain types and parameters.

To calculate the vehicle simulation, different parameters, which characterize the longitudinal simulated motion of the vehicle, have to be set. Therefore, the vehicle and powertrain parameters shown in Table 1 are used, to replicate the consumption of the *EDAG CityBot*. These parameters result in limitations for a maximum torque of $M = 1400$ Nm and a maximum speed of $v = 62.88$ km/h before reaching the field weakening region. All vehicles are executed to not exceed these values.

2.1. Intelligent Controlled Vehicle Modelling

For this paper, the approach by Eichenlaub et al. [13,14] is used. This approach uses state-of-the-art speed and headway control modes with target speeds v_{mode1} and v_{mode2}. These target speeds are extended with an anticipatory speed mode v_{mode3}. The speed control mode is modeled for this approach with $v_{\text{mode1}} = v_{\text{allowed}}$, with v_{allowed} being the allowed speed on the current lane of the ego vehicle. The headway control mode v_{mode2} is executed as shown in Equation (4).

$$v_{\text{mode2}} = v_e + \frac{1}{\tau_v}\left(v_l - v_e - \frac{1}{\tau_d}(d_0 + h_{\text{set}} v_e - d_t)\right) \tag{4}$$

Here, v_e is the current speed of the ego vehicle and v_l the actual speed of the leader vehicle. Thus, τ_v and τ_d are the time constants that can be parametrized for the control approach, d_0 and d_t are the actual and desired distance to the leading vehicle, h_{set} the target time gap.

Using V2X-information, an AI-based model, which is explained in detail in Eichenlaub et al. [14], predicts the speed trajectory of the upcoming traffic situation. The target speed for the anticipatory speed mode v_{mode3} is calculated by including the predicted information as shown in Equation (5). The lowest target speed of the three-speed modes is used as the target speed for the ego vehicle for the next time step.

$$v_{\text{mode3}} = \begin{cases} \frac{1}{N_{\text{pr}}} \sum_{j=t+\Delta t}^{t+N_{\text{pr}}} \hat{v}_l & \text{für dist.} < 150 \text{ m} \\ \\ \frac{1}{N_{\text{pr}}} \sum_{j=t+\Delta t}^{t+N_{\text{pr}}} \hat{v}_e & \text{otherwise} \end{cases} \tag{5}$$

Here, N_{pr} are the steps of the prediction horizon and Δt the step size of the prediction horizon. The speed $\hat{v}$ is the predicted speed for time step N_{pr}.

The chosen set speed is processed by a suitable PI controller, which is parameterized to guarantee safety by also resulting in a favorable dynamic behavior.

To also take into account the dynamic behavior of an electric powertrain, a first-order lag plant model is implemented with $\tau = 0.5$ s.

The results in Eichenlaub et al. [13,14] show that this control approach reduces the consumption of a vehicle in urban areas by up to 7.1% in comparison with not including the anticipatory speed mode v_{mode3}. It is also mentioned that the energy saving results not from a reduced mean speed, but from anticipated early speed reduction and by avoiding unnecessary acceleration.

In Figure 3 the control loop by Eichenlaub et. al. is displayed. The different types of information are explained and processed in the prediction model. With this information, the speed target v_{set} is calculated according to Equations (4) and (5). With a standard PI controller, the set acceleration a_{set} is calculated, which is processed within the vehicle model. This contains the vehicle dynamics and the powertrain model. The output of this is the energy demand E_cons and the applied vehicle speed v_{ego}. For more details refer to Eichenlaub et al. [13,14].
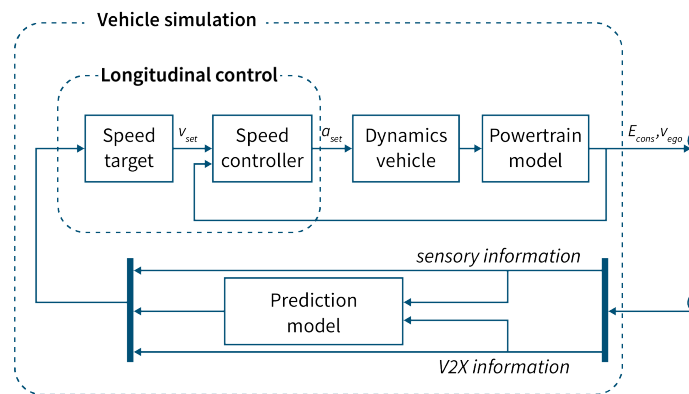

Figure 3. Vehicle simulation for an ICV with control approach.

2.2. Human Controlled Vehicle Modelling

To imitate a human driver, the Enhanced Intelligent Driver Model (EIDM) is used [26]. It is based on a basic car following model, the Intelligent Driver Model (IDM) [27], but also considers discontinuities like, for example, reaction times before braking or the different driving behavior with smaller or bigger gaps between vehicles. The IDM calculates the desired acceleration a_{IDM} with Equation (6).

$$a_{\mathrm{IDM}}(t + \Delta t) = a_{\max}\left[1 - \left(\left(\frac{v_{n-1}(t)}{v_0(t)}\right)^{\delta} - \left(\frac{s_{n-1}^*(t)}{s(t)}\right)^2\right)\right] \tag{6}$$

With $a_{\max}$ being the maximum speed, $s_{n-1}^*(t)$ being the desired and $s(t)$ the actual gap between ego and leader vehicle. Also, δ shows the acceleration exponent, $v_{n-1}(t)$ the actual velocity of the ego vehicle and v_0 the desired velocity.

The EIDM also uses a_{IDM} but additionally takes a Constant Acceleration Heuristic $a_{\mathrm{CAH}}(t)$ into account, which is shown in Equation (7).

$$a_{\mathrm{CAH}}(t) = \begin{cases} \frac{v_{n-1}^2 \tilde{a}_n}{v_n^2 - 2s(t)\tilde{a}_n} & v_n(v_{n-1} - v_n) \leq \\ & \quad -2s(t)\tilde{a}_n \\ \tilde{a}_n - \frac{(v_{n-1}-v_n)^2 \Theta}{2s(t)} & \text{otherwise} \end{cases} \tag{7}$$

$$\Theta = \begin{cases} 0 & v_{n-1} - v_n < 0 \\ 1 & v_{n-1} - v_n \geq 0 \end{cases} \tag{8}$$

$$\tilde{a}_n = \min(a_n(t), a_{\max}) \tag{9}$$

Here. v_n is representing the velocity and a_n the acceleration of the leader vehicle. Equations (8) and (9) form another acceleration option for the EIDM as shown in Equation (10).

$$a_{\mathrm{EIDM}} = (1 - c_{\mathrm{ACC}})a_{\mathrm{IDM}} + c_{\mathrm{ACC}} \\ \left[a_{\mathrm{CAH}} + b \tanh\left(\frac{a_{\mathrm{IDM}} - a_{\mathrm{CAH}}}{b} \right) \right] \tag{10}$$

The parameter c_{ACC} reflects the so-called coolness parameter, which sets the tendency to drive at higher speeds and lower distances. The final set acceleration a_{ACC} is displayed with a_{IDM} if $a_{\mathrm{IDM}} > a_{\mathrm{CAH}}$ otherwise a_{EIDM} is selected.

In addition to this description of the longitudinal motion of the EIDM, there are other minor enhancements in comparison to the IDM, which relate to reaction times, reaction on changing speed limits and turning speeds for corners. These improvements are accompanied by a further large number of variables, which can be set individually to adapt the driving behavior of the simulated driver.

To imitate a broad variety of different driving styles by different drivers, some characteristic parameters of the EIDM are chosen randomly out of a range of values. The varied parameters represent the drivers' imperfection σ related to the car following model, which takes on values between 0.011 and 0.985, and the time headway τ representing the reaction time of a driver, which takes on values between 0.54 and 1.128. All other variables are set to the SUMO default values. This value selection results in a realistic traffic scenario as shown in Eichenlaub et al. [14], by taking into account different driving styles.

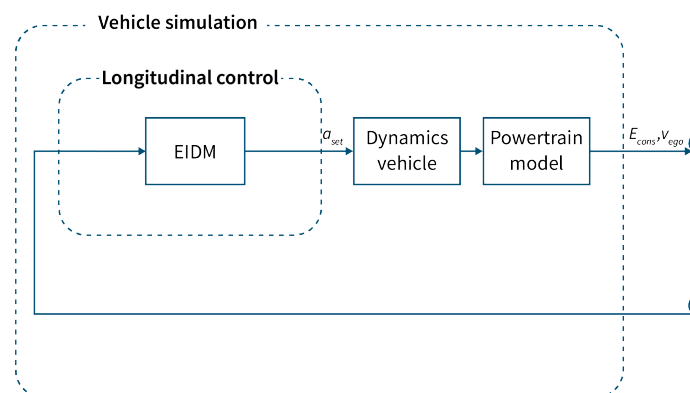The vehicle simulation for the HCV is shown in Figure 4.

Figure 4. Vehicle simulation for a HCV with EIDM.

3. Experimental Approach

Due to the high complexity of urban traffic, the impact of a vehicle on its surroundings is difficult to quantify.

Urban traffic provides a lot of dynamic and complex traffic scenarios, which are primarily defined by high traffic densities. These high traffic densities and the high percentage of roads, where overtaking is not allowed or possible, form vehicle queues.

For a quantification approach to the impact of a vehicle on its surrounding traffic, fixed system boundaries around the vehicle need to be set. In this paper, the following system boundaries are determined.

It is assumed, that a vehicle just has a minor or no impact on the vehicles in front, which sets the first boundary at its front end.

In real urban traffic, following vehicles change frequently within a driven route, but in most situations, due to high traffic densities, at least one direct following vehicle is

present. Therefore, urban traffic can be interpreted by vehicle queues forming due to vehicle following situations. Even though, vehicles, their distances, and positions within the queue change frequently. To simplify and summarize the impact of all different following vehicles during a journey, in this paper, a fixed group of following vehicles is implemented. These vehicles follow the leading vehicle during the whole route. This represents one possible following situation in an urban traffic scenario.

Because it is assumed that the influence of the leader is getting smaller with an increased distance backward, the second system boundary is set ten following vehicles behind the leader vehicle. This assumption is confirmed within the results in Section 4.

Vehicle queues can be stopped, separated and changed in urban traffic scenarios by right-of-way situations, other traffic-related situations, or traffic lights. These impacts on the queue have similar effects on the vehicle queue's behavior. These situations are separating the vehicle queue at a certain point and will reduce the impact of a leading vehicle to the following vehicles behind this point.

These situations can be summarized as general interrupting situations. In this paper, these are only executed with traffic lights because they allow traffic situations that are plannable and comprehensible. Therefore, all other traffic participants, which cause all other interrupting situations, can be excluded from the following investigation.

Thus, the traffic scenario is reduced to the described vehicle queue. The vehicles start 5 s after each other, to overcome the starting process of a vehicle's trajectory. The leader vehicle can be executed as ICV and HCV. All the following vehicles represent the surrounding traffic and are executed as HCVs. The resulting traffic scenario with the leading vehicle and the followers from i = 1 to i = 10 is shown in Figure 5.

Figure 5. Vehicle queue for car following scenario.

To avoid the influence of specific combinations of traffic light intervals that cause certain queue interruption events, all investigations in this paper are executed 100 times with a different start time of 3 s between each simulation. This number of simulations tries to exclude the influence of outliers, which would result from specific traffic light phase combinations.

To maintain an intact system with ten queued vehicles, overtaking is not possible, and just one-lane roads are selected for the chosen scenario. This can be justified by considering the share of one-lane roads within the shown traffic environment in Figure 2. In this traffic scenario, the share of one-lane roads amounts to 80%, so the focus on this type of street is reasonable.

For the investigation of the described system and the leading vehicle's impact on the followers, a one-lane route is selected as exemplary for typical urban traffic. The scenario (R) is shown in Figure 2.

The scenario (R) has a distance of 1.20 km with three traffic lights at 0.13 km, 0.54 km and 0.75 km. These have fixed but not equal light phases, which generate a multitude of different combinations.

4. Results

The impact of the leader vehicle is evaluated by the position of the vehicle within the vehicle queue and by the distance to the leader vehicle, regardless of the position within the queue. These results, therefore, include both the impact caused by the distance to the leader and caused by the vehicles between the leader vehicle and the specific follower HCV.

4.1. Investigation by Number of Vehicles to Leader

In Figure 6a, the distribution of consumption of each vehicle within the vehicle queue is shown. The red line is marking the median consumption of a HCV over the given scenario (R) without being inflicted by an ICV.
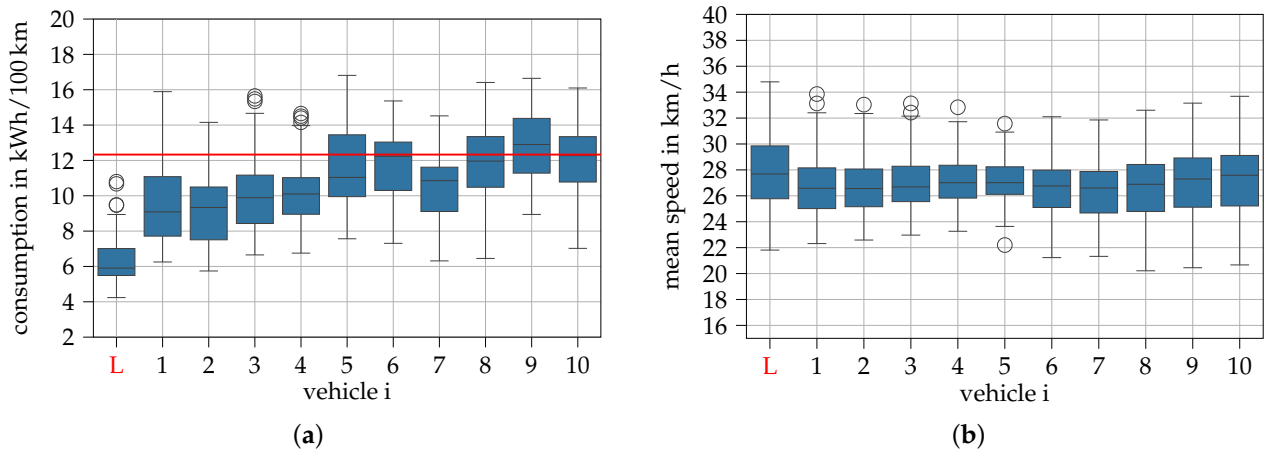

Figure 6. Consumption and mean speed for the ICV lead (vehicle L) vehicle queue with all HCV followers (vehicle 1–10) in scenario (R), with the red marked average consumption for an HCV in this scenario. (**a**) Energy consumption; (**b**) Mean speed.

The leading vehicle, which is controlled as an ICV, shows a significant lower energy consumption in all cases, compared to the median consumption of an HCV. This confirms the results of Eichenlaub et al. [13,14].

Also, the following vehicles i = 1 to i = 4 are showing in most cases a lower consumption, which can be interpreted as a verifiable positive impact in terms of consumption of the leading vehicle to the first four following vehicles. The median consumption is showing a reduction in consumption of 22% to 16% for this traffic scenario for vehicles i = 1 to i = 4 compared to the median consumption of an HDV. The occasionally measured values of these vehicles, which are significantly above the median consumption of the vehicle under consideration and also above the red marked median consumption, can be traced back to situations where the vehicle queue is split up early during the route. In these cases, the distances and the impact of the ICV leader are lowered.

From the following vehicles i = 5 to i = 10 the consumption converged to the median consumption of an HCV on this route. This group of vehicles can be interpreted as the vehicles, which the ICV leader has in most cases just minor influences on, due to larger distances to the intelligent controlled vehicle.

The fluctuations in the values in the second group of follower vehicles, which include vehicles i = 5 to i = 10, can be explained by two reasons. At first, the randomness in the parametrization of the HCV, which results in a variety of driving styles, and therefore, also in a variety of different consumption results. Also, different queuing situations could cause this outcome. For example, the slightly lower consumption for vehicle i = 7 can appear due to a specific combination of traffic light phases, which interrupts the vehicle queue at this point.

It can be assumed, that with an even bigger number of simulations, the convergence towards the red marked median value would be more obvious. Also, the focus on one specific traffic scenario can cause these minor fluctuations for specific vehicles. Because in this paper the fluctuations of the minor impacted vehicles is not relevant, the results for the last six vehicles within the queue can nevertheless be categorized as unambiguous in order to quantify the influence of a leader vehicle.

The mean speed for all vehicles within the described traffic scenario is shown in Figure 6b. It is clear that the mean speed for all vehicles, regardless the control design, is very similar. This indicates, that the energy savings, shown in Figure 6a are not expected to be caused by

lower mean speeds but by less acceleration situations, caused by the predictive element of the ICV. This behavior will be continued to the following vehicles, which will adapt these actions.

4.2. Investigation by Distance to Leader

The previous results are an implication for a positive impact of the ICV to the surrounding traffic for at least four vehicles behind. As mentioned, the consumption is interfered not only by the number of vehicles between itself and the leading vehicle but also by the distance to the leading vehicle. To quantify the impact of the leading vehicle by distance, in Figure 7, the appearances of consumption over the distance to the leading vehicles is shown for both leading vehicle types, the HCV in Figure 7a and the ICV in Figure 7b. In these Figures, the order of the vehicles is neglected.
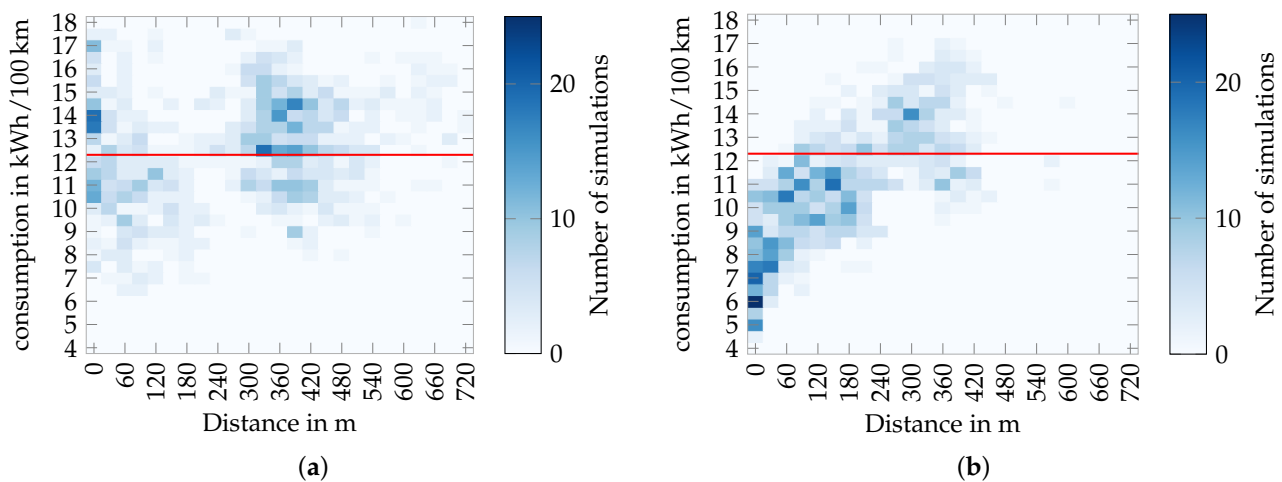
Figure 7. Heat map of the average consumption in scenario (R) for all executed simulations, with the red marked average consumption for an HCV in this scenario. (**a**) leading vehicles HCV; (**b**) leading vehicles ICV.

For the HCV leader in Figure 7a, the distribution of the consumption stays relatively constant throughout the distance to the leader vehicle. In contrast to this, for the ICV leader in Figure 7b the follower vehicles are showing a steady increase in consumption with increased distance up to a distance of 250 m. This confirms and explains the results of the consideration of the following vehicles in Figure 6a. After a distance of about, 250 m the following vehicles reach the median consumption of an HCV vehicle for this route, regardless of the leader vehicle. This distance can be stated as the maximum distance of influence for this scenario.

For both types of leader vehicles, an interval of distance with a lower number of drives with the corresponding consumption can be observed at a distance of approximately 200 m. This is more significant for the HCV leader vehicle but can also be seen for the ICV leader. This gap can be caused by the chosen traffic scenario and could be a result of just investigating one specific scenario. This could also be the reason for the fluctuations in Figure 6a for later vehicles within the vehicle queue with the ICV leader. It is part of further research to investigate more traffic scenarios to confirm this hypothesis.

5. Conclusions

In this work, the influence of an ICV on a mixed traffic scenario is quantified. Therefore, a characteristic urban traffic scenario has been selected, and necessary assumptions were formulated. Even though these results are just based on one exemplary scenario, the results give an impression of the impact of an ICV on urban traffic.

The results, which depend on the models used for HCV and ICV, need to be interpreted in this context. This is countered by the fact that a validated HCV model was used, which

is based on real driving data and a state-of-the-art intelligent longitudinal control, which is representative of such systems.

Even though the absolute values may differ with other models, the main objective, which is a significant influence of ICVs in mixed traffic, can be seen as general for a wide range of intelligent longitudinal control systems.

The results show that an efficiently controlled vehicle can have a significant area of influence in relation to other traffic participants in a mixed-traffic environment. This can be quantified by up to four follower vehicles or around 250 m behind the vehicle under consideration. This could imply that with an increasing number of autonomous ICVs, the energy consumption of a certain mixed vehicle fleet could be reduced even more than just by the energy saving of the autonomous ICV but also by having a positive impact on surrounding HCV traffic.

With the shown results, the energy saving of a vehicle fleet, which includes ICVs, can be derived for other traffic situations.

In the future, these results have to be confirmed by further investigations, e.g., by setting even bigger system boundaries, concerning a whole vehicle fleet or a part of a city, where ICVs are operating in mixed traffic. Also, the impacted radius by increasing the market share of ICV to mixed traffic is another topic that should be considered in future investigations, to validate and extend the shown results.

References

1. Fagnant, D.J.; Kockelman, K. Preparing a nation for autonomous vehicles: Opportunities, barriers and policy recommendations. *Transp. Res. Part A Policy Pract.* **2015**, *77*, 167–181. [CrossRef]
2. Al-Turki, M.; Ratrout, N.T.; Rahman, S.M.; Reza, I. Impacts of Autonomous Vehicles on Traffic Flow Characteristics under Mixed Traffic Environment: Future Perspectives. *Sustainability* **2021**, *13*, 11052. [CrossRef]
3. Lücke, N. Status Quo des Autonomen Fahrens: Die Zukunft hat Bereits Begonnen. 2019. Available online: https://www.vdi.de/themen/mobilitaet/autonomes-fahren/status-quo-des-autonomen-fahrens (accessed on 11 January 2024).
4. Azam, M.; Hassan, S.A.; Che Puan, O. Autonomous Vehicles in Mixed Traffic Conditions—A Bibliometric Analysis. *Sustainability* **2022**, *14*, 10743. [CrossRef]
5. Eßer, A. *Realfahrtbasierte Bewertung des ökologischen Potentials von Fahrzeugantriebskonzepten*; Shaker: Düren, Germany, 2021. [CrossRef]
6. Morando, M.M.; Tian, Q.; Truong, L.T.; Vu, H.L. Studying the safety impact of autonomous vehicles using simulation-based surrogate safety measures. *J. Adv. Transp.* **2018**, *2018*, 6135183. [CrossRef]
7. Talebpour, A.; Mahmassani, H.S. Influence of connected and autonomous vehicles on traffic flow stability and throughput. *Transp. Res. Part C Emerg. Technol.* **2016**, *71*, 143–163. [CrossRef]
8. Dey, K.C.; Yan, L.; Wang, X.; Wang, Y. A Review of Communication, Driver Characteristics, and Controls Aspects of Cooperative Adaptive Cruise Control (CACC). *IEEE Trans. Intell. Transp. Syst.* **2016**, *17*, 491–509. [CrossRef]
9. Yang, H.; Jin, W.L. A control theoretic formulation ofgreen driving strategies based on inter-vehicle communications. *Transp. Res. Part C Emerg. Technol.* **2014**, *41*, 48–60. [CrossRef]
10. Walz, F.J. *Modellbasierte Prädiktive Längsdynamikregelung für Künftige Fahrerassistenz- und Automatisierungssysteme*; Karlsruhe Institute of Technology: Karlsruhe, Germany, 2024. [CrossRef]
11. Morlock, F.; Sawodny, O. An economic model predictive cruise controller for electric vehicles using Gaussian Process prediction. *IFAC-PapersOnLine* **2018**, *51*, 876–881. [CrossRef]

12. Patella, S.; Scrucca, F.; Asdrubali, F.; Carrese, S. Carbon Footprint of autonomous vehicles at the urban mobility system level: A traffic simulation-based approach. *Transp. Res. Part D Transp. Environ.* **2019**, *74*, 189–200. [CrossRef]
13. Eichenlaub, T.; Rinderknecht, S. Anticipatory Longitudinal Vehicle Control using a LSTM Prediction Model. In Proceedings of the 2021 IEEE International Intelligent Transportation Systems Conference (ITSC), Indianapolis, IN, USA, 19–22 September 2021; pp. 447–452. [CrossRef]
14. Eichenlaub, T.; Heckelmann, P.; Rinderknecht, S. Efficient Anticipatory Longitudinal Control of Electric Vehicles through Machine Learning-Based Prediction of Vehicle Speeds. *Vehicles* **2023**, *5*, 1–23. [CrossRef]
15. Lopez, P.A.; Behrisch, M.; Bieker-Walz, L.; Erdmann, J.; Flotterod, Y.-P.; Hilbrich, R.; Lucken, L.; Rummel, J.; Wagner, P.; WieBner, E. Microscopic Traffic Simulation using SUMO. In Proceedings of the 2018 21st International Conference on Intelligent Transportation Systems (ITSC), Maui, HI, USA, 4–7 November 2018; pp. 2575–2582.
16. Huang, J. Vehicle longitudinal control. In *Handbook of Intelligent Vehicles*; Springer: London, UK, 2012; pp. 167–190.
17. Rajamani, R. *Vehicle Dynamics and Control*; Springer Science & Business Media: New York, NY, USA, 2011.
18. Syrnik, R. Untersuchung der Fahrdynamischen Potenziale eines Elektromotorischen Traktionsantriebs. Ph.D. Thesis, Technische Universität München, München, Germany, 2015.
19. Short, M.; Pont, M.J.; Huang, Q. Simulation of vehicle longitudinal dynamics. In *Safety and Reliability of Distributed Embedded Systems*; Technical Report ESL 04-01; 2004. Available online: https://www.researchgate.net/publication/329588123_Simulation_of_Vehicle_Longitudinal_Dynamics (accessed on 20 August 2024).
20. Esser, A.; Eichenlaub, T.; Schleiffer, J.E.; Jardin, P.; Rinderknecht, S. Comparative evaluation of powertrain concepts through an eco-impact optimization framework with real driving data. *Optim. Eng.* **2021**, *22*, 1001–1029. [CrossRef]
21. Bao, D.W.; Zhou, J.Y.; Zhang, Z.Q.; Chen, Z.; Kang, D. Mixed fleet scheduling method for airport ground service vehicles under the trend of electrification. *J. Air Transp. Manag.* **2023**, *108*, 102379. [CrossRef]
22. Kraus, M.; Harkort, C.; Wuebbolt-Gorbatenko, B.; Laumann, M. Verschmelzung von Antrieb und Fahrwerk für einen People Mover. *ATZ Automob. Z.* **2018**, *120*, 48–53. [CrossRef]
23. Peichl, T.; Rinderknecht, S. Parameter Study on the Influence of Driving Cycle and Powertrain Parameterization on Fuel Consumption of wheel-hub driven Vehicles. In *Proceedings of the Dritev 2024*; VDI Verlag: Düsseldorf, Germany, 2024; pp. 141–158. [CrossRef]
24. Rieger, P.; Heckelmann, P.; Peichl, T.; Schwindt-Drews, S.; Theobald, N.; Crespo, A.; Oetting, A.; Rinderknecht, S.; Abendroth, B. A Multidisciplinary Approach for the Sustainable Technical Design of a Connected, Automated, Shared and Electric Vehicle Fleet for Inner Cities. *World Electr. Veh. J.* **2024**, *15*, 360. [CrossRef]
25. Barckmann, J.; Herchet, H.; Körbel, G. Mobility Concept of a Street Robot. *ATZ Worldw.* **2020**, *122*, 16–21. [CrossRef]
26. Salles, D.; Kaufmann, S.; Reuss, H.-C. Extending the Intelligent Driver Model in SUMO and Verifying the Drive Off Trajectories with Aerial Measurements. In Proceedings of the SUMO User Conference, Virtual Event, 26–28 October 2020. [CrossRef]
27. Treiber, M.; Helbing, D. Realistische Mikrosimulation von Straßenverkehr mit einem einfachen Modell. In Proceedings of the Symposium Simulationstechnik (ASIM 2002), Rostock, Germany, 10–13 September 2002.